#4452 - Revision 2

Rapidcreekite in the sulfuric acid weathering environment of Diana Cave, Romania

Bogdan P. Onac[1,2*], Herta S. Effenberger[3], Jonathan G. Wynn[1], Ioan Povară[4]

[1]Department of Geology, University of South Florida, 4202 E. Fowler Ave., SCA 528, Tampa, FL 33620, USA

[2]Emil Racoviță Institute of Speleology / Department of Geology, Babeș-Bolyai University, Kogălniceanu 1, 400084, Cluj-Napoca, Romania

[3]Institute of Mineralogy and Crystallography, University of Wien, Althanstrasse 14, A-1090 Wien, Austria

[4]Emil Racoviță Institute of Speleology, Frumoasă 31, 010986 Bucharest, Romania

* Corresponding author: B.P. Onac (bonac@usf.edu)

Abstract

The Diana Cave in SW Romania develops along a fault line and hosts a spring of hot (T_{avg} = 51ºC), sulfate-rich, sodium-calcium-chloride bearing water of near-neutral pH. Abundant steam and H_2S rises from the thermal water to condensate on walls and ceiling of the cave. The sulfuric acid produced by H_2S oxidation/hydrolysis causes a strong acid-sulfate weathering of the cave bedrock generating a sulfate-dominated mineral assemblage that includes rapidcreekite, $Ca_2(SO_4)(CO_3)\cdot 4H_2O$ closely associated with gypsum and halotrichite group minerals. Rapidcreekite forms bundles of colorless tabular orthorhombic crystals elongated along [001] and reaching up to 1.5 mm in length. For verifying the hydrogen bond scheme and obtaining crystal

chemical details of the carbonate group a single-crystal structure refinement of rapidcreekite was performed. Its unit-cell parameters are: *a* 15.524(2), *b* 19.218(3), *c* 6.161(1) Å; *V* 1838.1(5) Å^3, *Z* = 8, space group *Pcnb*. Chemical composition (wt.%): CaO 35.65, SO_3 24.97, CO_2 13.7, H_2O 23.9, Na_2O 0.291, MgO 0.173, Al_2O_3 0.07, total 98.75 %. The empirical formula based on 7 non-water O atoms p.f.u. is: $Ca_{1.98}Na_{0.029}Mg_{0.013}Al_{0.004}(S_{0.971}O_4)(C_{0.97}O_3)\cdot 4.13H_2O$. The $\delta^{34}S$ and $\delta^{18}O$ values of rapidcreekite and other cave sulfates range from 18 to 19.5‰ CDT and from -9.7 to 7.8‰ SMOW, respectively, indicating that the source of sulfur is a marine evaporite and that during hydration of the minerals it has been an abundant ^{18}O exchange with percolating water but almost no oxygen is derived from $O_{2(aq)}$. This is the first description of rapidcreekite from a cave environment and one of the very few natural occurrences worldwide. It also reports on the mineral stability and solubility, parameters considered critical to understand the co-precipitation of carbonates and sulfates, a process that has wide applications in cement industry and scaling prevention.

Keywords: rapidcreekite, acid-sulfate weathering, hydrogen bond scheme, carbonate group, $\delta^{34}S$-$\delta^{18}O$ values, Diana Cave, Romania

Introduction

Sulfates are the largest group among cave minerals, with 89 species forming in a variety of settings (Hill and Forti 1997; Onac and Forti 2011a, b). Of these, only gypsum, epsomite, and mirabilite may be considered common for the cave environments, with gypsum perhaps the second most frequent cave mineral after calcite (Onac 2012). The majority of the other sulfates only occur under very particular settings, such as in caves located nearby ore deposits or thermo-mineral water sources and in areas with abundant post-volcanic activities.

Previous mineralogical studies on cave sulfates precipitated in sulfidic-rich steam condensate alteration environments are known from many locations worldwide. Spallanzani (1797) provided the first written report describing alunogen $Al_2(SO_4)_3(H_2O)_{12}\cdot 5H_2O$, halotrichite $Fe^{2+}Al_2(SO_4)_2\cdot 22H_2O$, and an unidentified iron sulfate from the Alum Cave (Vulcano Island, Sicily). More recent accounts on the mineralogy of this unique volcanic cave highlights the presence of 22 sulfate minerals (Forti et al. 1996; Demartin et al. 2010). Rodgers et al. (2000) report a complex suite of minerals from another non-limestone cavity (Ruatapu Cave, New Zealand) developed in hydrothermally altered vitric tuffs. When acid sulfate weathering takes place in limestone caves, however, the mineralogy is dominated by gypsum. This is the case for the famous, presently active sulfidic-rich cave systems from Frasassi and Acquasanta (Italy; Galdenzi et al. 2003, 2010) and Villa Luz (Mexico; Hose et al. 2000). When the lithology exposed within carbonate caves varies, the sulfidic steam condensate mineralogy may be complex. Examples falling under this category include a number of caves from France, Romania, and Greece (Povară et al. 1972; Diaconu and Medeşan 1973; Audra and Hobléa 2007; Onac et al. 2009a; Lazarides et al. 2011).

Rapidcreekite, ideally $Ca_2(SO_4)(CO_3)\cdot 4H_2O$, has only been found in nature at a very few localities; usually it is in association with gypsum and a carbonate mineral. The mineral was originally described by Roberts et al. (1986) from an iron-rich deposit in the Rapid Creek area (Yukon, Canada), then three years later by Walenta and Dunn (1989) from the Johann Mine (Black Forest, Germany) under a completely different setting (U-Co mineralization zone). In this later occurrence, rapidcreekite is associated primarily with camgasite, calcite, monohydrocalcite, and gypsum; iron containing minerals are absent there. Further localities are two mines in Norway and Germany, respectively, and a possible cave location in Czech Republic (Raade 1989; Rüger et al. 1995; Žák et al. 2010). Synthetic rapidcreekite has also been identified as an intermediate phase during desalinization studies from solutions having a low carbonate to sulfate ratio (Dydo et al. 2003; Schausberger et al. 2009). Rapidcreekite was recently reported as the main hydration product in a ternary cement system where it formed via ettringite carbonation (Martínez-Romírez and Fernández-Carrasco 2012).

Early in 2008, the mineral assemblages of a number of caves located along the Cerna Valley (SW Romania) and affected by ascending sulfide-rich thermo-mineral waters were investigated by Onac et al. (2009a), reporting the probable presence of rapidcreekite in the Diana Cave. The present paper describes this new occurrence of rapidcreekite in detail. Its discovery in the environment of the Diana Cave is significantly different from the other known localities mentioned above.

Diana Cave settings

The Diana Cave is located in southwestern Romania in the old center of Băile Herculane, a famous thermal spa founded more than 2000 years ago (Povară 2001). It opens on the right bank of the Cerna River at ~7 m above its thalweg and consists of a 22 m, V-shaped cave passage at the

88 far end of which the Diana thermal spring emerges (Povară et al. 1972). The mean annual cave
89 temperature is 22ºC, and relative humidity is 100% year around, except for the cold periods, when
90 outside dry air enters the cave and causes a drop of the water vapor partial pressure (85-95%) and
91 thus evaporative conditions prevail in the cave.
92 The regional geology is rather complex; its relationship with the karst of the Cerna Valley has
93 been described in details elsewhere (Schmid et al. 1998; Povară et al. 2008; Wynn et al. 2010).
94 Relevant to the current research is that the cave passage formed along the Diana Fault; this enables
95 the contact between the Late Jurassic nodular limestone and the Early Cretaceous gray-black Iuta
96 marls (Năstăseanu 1980).
97
98 **Diana Cave Spring**
99 As early as 1881, the thermal water (mean temperature ~51 ºC; Povară et al. 2008) of Diana's
100 Spring was confined (for balneotherapy purposes) within the cave by a dam built at its entrance. In
101 the early 70's, a narrow cave passage heading SE was enlarged to drain the thermal water outside
102 in a retention basin, from where it is pumped in a series of thermal baths. During this work all cave
103 passages were enlarged and the walls, especially where marl crops out, were reinforced using
104 concrete. Consequently, the original cave morphology was altered and the mineral deposits that
105 had precipitated over the cave walls (in form of efflorescences and crusts) were hidden behind the
106 concrete wall. Since the construction, however, the acid sulfate corroded the concrete and the cave
107 walls are now exposed on restricted areas allowing for sample collection.
108 Diana Cave hosts two thermal springs (referred as Diana 1 and 2, respectively; Povară et al.
109 2008). The total dissolved solids of the waters is around 5700 mg/L and contain on average 1392.5
110 mg/L Na^+, 725 mg/L Ca^{2+}, 3370 mg/L Cl^-, and abundant H_2S degasses into the cave atmosphere.

The sodium-calcium-chloride type thermo-mineral water has a nearly neutral pH (~6.5), and its total sulfide and sulfate concentration is 37 and 92 mg/L, respectively (Marin 1984; Wynn et al. 2010). The Diana Springs show excess concentrations of methane in its thermal water (Cosma et al. 2008), which enables a nearly complete thermochemical sulfate reduction (TSR). This process generates high $\delta^{34}S$ values (27.2 ‰) of SO_4^{2-} in the solution and high dissolved sulfide concentrations (>37 mg/L as S^{2-}) with a $\delta^{34}S$ value that takes on the approximate isotopic signature of the total dissolved S (mean +17.4‰) (Wynn et al. 2010; Onac et al. 2011). From the spring hydrochemistry, temperature, regional hydrogeology, and sulfur isotopic signature, Povară et al. (2008) and Onac et al. (2011) concluded that the thermal waters around Băile Herculane Spa (including the Diana Springs) represent deeply circulating meteoric waters that are upwelling along stratigraphic boundaries or faults.

The milky color of the water flowing along the NW-SE passage results from suspended elemental sulfur and sub-millimeter thin gypsum rafts (not larger than 60 cm^2) precipitating at the water-air interface. The abundant sulfidic steam released by the hot waters emerging from the Diana Springs condenses on the colder bedrock surface. Subsequent oxidation/hydrolysis of sulfides creates sulfuric acid solutions (pH between 3 and 4.5), which react with the bedrocks to form a variety of sulfates and controls the resulting cave steam-heated (also called acid-sulfate) weathering environment of the Diana Cave.

The Diana Cave mineral association

The mineralogical investigations in the Diana Cave were carried out in two distinct periods. The first one occurred in the early 70's when Povară et al. (1972) briefly reported on the presence of elemental sulfur, gypsum, and 'halotrichite' in a general presentation of the caves affected by

thermal waters in the lower section of the Cerna Valley. A year later, a detailed study of the acicular-prismatic crystals originally described as 'halotrichite', proved to be in fact pickeringite (Diaconu and Medeşan 1973). The authors suggested that the mineral precipitated from the reaction between the acidic thermal waters and the marls on the cave floor. In another study, Diaconu (1974) described the world's first cave occurrence of anhydrite from the same cave.

The mineralogical investigations revived in 2007 when the lead author received a 3-year grant to study the sulfuric acid caves along the Cerna Valley. Due to its active sulfidic environment, the Diana Cave is a central point of research in the region. In two consecutive papers, Onac et al. (2009a and b) confirmed the presence of halotrichite; in addition apjohnite, epsomite, tamarugite, as well as rapidcreekite were identified.

Neither tamarugite nor rapidcreekite were described from carbonate karst caves so far, thus prompting us for more elaborate studies; one is dedicated to tamarugite (Puşcaş et al. 2013) and the present one to rapidcreekite.

Samples and methods

Nine samples of transparent to white or yellowish-brown efflorescences and damp aggregates were collected from exposed sections of the cave wall (middle and lower part) at the far end of the Diana Cave and from the upper part of the concrete piers that cover the man made waterway, respectively. The patchy efflorescences in which rapidcreekite was later identified always form directly over the weathered limestone and are intimately associated with fibrous gypsum crystals. In the lowermost part of the walls and on the floor (within the same cave section) directly overlying the weathered marls, halotrichite group minerals were found. The presence of rapidcreekite was documented in two of these nine samples.

158 Chemical analyses were performed using a JEOL 8900R Superprobe electron microprobe
159 (EMPA) instrument at the Department of Earth Sciences, Florida International University.
160 Analytical conditions were: 15 kV, 5 and 10 nA, defocussed electron-beam diameter of 30 μm
161 (sample was moved to avoid decomposition of the mineral under the beam), WDX: peak count-
162 time 60 s, background count-time 15 s). Apatite (Ca), anhydrite (SO_3), Diopside2 (MgO),
163 Kaersutite2 (K_2O), and PlagAn65 (Na_2O, Al_2O_3) served as standards. The CO_2 and H_2O content in
164 the samples was calculated by means of thermogravimetric method using a Netzsch thermal
165 apparatus with the following working conditions: sample weight 1.5 g, heating rate 10º/min, and
166 temperature range 20 to 1000 ºC). Computation of the empirical formula was performed using
167 MINCALC-V5 software (Bernhardt 2010).
168 The SEM investigations were carried out on a JEOL 6490 LV operated in low vacuum mode
169 and equipped with an EDS analytical system in the Lisa Muma Weitz Imaging Core Laboratories
170 (University of South Florida).
171 Sulfur and oxygen isotopic composition of SO_4^{2-} in bulk sulfates and in rapidcreekite (hand
172 picked under the microscope) was measured in the Stable Isotope Laboratory of the Department of
173 Geology (USF) on a Delta V Isotope Ratio Mass Spectrometer (IRMS) using a Costech Elemental
174 Analyzer and a Temperature Conversion Elemental Analyzer, respectively, coupled to the IRMS
175 following the methods described in Nehring et al. (1977), Grassineau et al. (2001), and Wynn et al.
176 (2010). The results were normalized to Cañon Diablo Troilite (CDT) and Vienna Standard Mean
177 Ocean Water (VSMOW) using $\delta^{34}S$ and $\delta^{18}O$ values of the two IAEA standards (International
178 Atomic Energy Agency, IAEA SO-5 ($\delta^{34}S$ = 0.5 ‰; $\delta^{18}O$ = 12 ‰) and IAEA SO-6 ($\delta^{34}S$ = -34.1
179 ‰; $\delta^{18}O$ = -11 ‰). The reproducibility between replicate standards in each run was estimated to
180 be better than ±0.1 and ±0.3 ‰ (1σ), respectively. Geochemical equilibrium modeling and

calculations of the saturation index of calcite (SI_{calc}) were completed using the geochemical speciation program PHREEQC (Parkhurst and Appelo 1999).

Results and discussion

Physical properties

Rapidcreekite appears either as transparent, euhedral to subhedral acicular crystals or, more commonly, in whitish clusters of flattened prismatic crystals with a silky lustre. Scanning-electron imaging of rapidcreekite reveals bundles of crystals flattened on {010} and elongated along [001] (Figs. 1a and b). A perfect cleavage is observed on {100}. Crystal length measurements range from 40 to 1500 μm ($\overline{X}$ = 321 μm, n = 107 individual crystals). Irregular and globular white mate aggregates were found growing upon the prismatic rapidcreekite crystals (Fig. 1b).

Chemical and isotopic composition

The average composition (in wt%) of rapidcreekite obtained from 7-point measurements on two crystals is CaO: 35.65, SO_3: 24.97, Na_2O: 0.291, MgO: 0.173, Al_2O_3: 0.07, CO_2: 13.7, and H_2O: 23.9 (total: 98.75). The empirical formula based on 7 non-water O atoms p.f.u. is $Ca_{1.98}Na_{0.029}Mg_{0.013}Al_{0.004}(S_{0.971}O_4)(C_{0.97}O_3)\cdot 4.13H_2O$, ideally, $Ca_2(SO_4)(CO_3)\cdot 4H_2O$. This composition is in accordance with the only analysis reported so far by Roberts et al. (1986) for the Yukon rapidcreekite.

Semi-quantitative EDS analyses taken at natural faces of the aggregates growing upon the rapidcreekite crystals show the presence of C, O, and Ca in an atomic ratio 1:1:1. This finding corresponds well with the observation from the experimental work of Dydo et al. (2003) and the

crystallization experiment of precipitating synthetic analogues of gypsum and vaterite via rapidcreekite by Bots (2011). Both studies reported the formation of carbonates (mainly vaterite and aragonite) along with rapidcreekite.

The isotopic composition ($\delta^{34}S$ and $\delta^{18}O$) of rapidcreekite and bulk sulfate minerals occurring as crusts and efflorescences is listed in Table 1. The data set is homogeneous, showing ^{34}S-enriched $\delta^{34}S$ values (18 to 19.5 ‰ CDT) whereas the $\delta^{18}O$ values range from -9.7 to -7.8 ‰ VSMOW.

X-ray experiments and refinement of the crystal structure

The crystal structure of rapidcreekite was determined by Cooper and Hawthorne (1996). However, the authors could not locate the H atoms during their final refinements and established the hydrogen-bond system based on crystal chemical considerations. For a detailed discussion of the shape of the carbonate group, to verify the hydrogen bond scheme, and for a confident identification of rapidcreekite from a karst cave, a precision single-crystal study was performed at the University of Vienna (for details see Table 2). The crystal structure was refined starting from the atomic coordinates given by Cooper and Hawthorne (1996). The increased accuracy is mainly based on the larger number of observed reflections due to the use of an area detector, which allowed establishment of the location of the H atoms in a difference Fourier summation and the refinement of their atomic coordinates. However, the quality of the available crystals and the accuracy of the X-ray data allowed only an approximate location of the H atoms. Although there is no doubt on the main features of the hydrogen bond scheme, the actual positions of the H atoms' electrons are only approximate given the superposition of the H atom with inaccuracies in the electron density map. As a consequence, some O-H bonds differ from the expected values detected by X-ray investigations. The final structural parameters of rapidcreekite are given in Table 3;

interatomic bond distances and the geometry of the hydrogen bonds in Table 4. Further details of the crystal structure investigation may be obtained from Fachinformationszentrum Karlsruhe, 76344 Eggenstein-Leopoldshafen, Germany (fax: +49-7247-808-666; e-mail: crysdata@fiz-karlsruhe.de) on quoting the deposition number CSD-425547.

The results of the structural refinement compare well with the former description by Cooper and Hawthorne (1996). The atomic arrangement is characterized by rows of edge sharing $Ca1O_6(O_w)_2$ and $Ca2O_6(O_w)_2$ coordination polyhedra linked among each other by corners forming layers parallel to (100). Each of the SO_4 and CO_3 groups share edges with a $Ca1O_6(O_w)_2$ and a $Ca2O_6(O_w)_2$ coordination polyhedron. The layers are linked by hydrogen bonds only. The hydrogen bonds postulated by Cooper and Hawthorne (1996) for the water molecules O_w2H_2, O_w3H_2 and O_w4H_2 were confirmed. However, for both the hydrogen bonds of the O_w1H_2 molecule there is only one acceptor O atom. For one of the hydrogen bonds of the O_w4H_2 molecule the bifurcated hydrogen bond is confirmed. For the bifurcated H bond the bond angles O—H$\overset{\triangle\triangle\triangle}{=\!=\!=}$O are 86 and 144° whereas the others vary between 157 and 169°. Within the accuracy of the structure refinement, the H atom involved in the bifurcated hydrogen bond has a planar coordination by the donor atom and the two acceptor atoms [sum of bond angles 357(4)°].

The carbonate group features an approximately trigonal planar surrounding. The average C—O bond length of 1.284 Å corresponds exactly with the mean value of 1.284(18) Å reported by Zemann (1981) for 102 accurately determined carbonate groups of mineral structures. Despite the fact that the carbonate group shares two O—O edges with the CaO_8 polyhedra, the O—C—O bond angles deviate only slightly: they are 118.67(12) and 118.34(13)° for the shared and 122.95(14)° for the unshared edges. Noteworthy is the aplanarity of the carbonate group; the C atom lays 0.0157(16) Å above the plane defined by the three coordinating oxygen atoms (Fig. 3). This

deviation is caused by the electrostatic influence of the four Ca atoms in the surrounding of the carbonate group. Only one Ca2 atom is located slightly above the oxygen-atom plane of the carbonate group [0.037(3) Å] whereas the further Ca2 and the two Ca1 atoms are significantly below this plane [0.687(2), 0.639(2), and 1.232(2) Å]. The deviation from planarity compares with those found in other carbonates like dolomite, bütschliite, or thaumasite with 0.018(1), 0.014(2), and 0.018(1) Å, respectively (Effenberger et al. 1981; Effenberger and Langhof 1984; Gatta et al., 2012).

The equivalent isotropic displacement parameters U_{equiv} of the Ca, S, and C atoms are 0.01621(9) to 0.01712(18) $Å^2$, those of the oxygen atoms belonging to the anion groups are slightly larger (0.0191(2) to 0.025(2) $Å^2$) but smaller as compared to those of the oxygen atoms belonging to the water molecules 0.0252(3) to 0.0296(3) $Å^2$. The ratios longest/shortest axes of the principal mean square atomic displacement of U_{ij} are small for the Ca, S, and C atoms (1.140 to 1.295) but significantly larger for the oxygen atoms belonging to the anion groups (1.455 to 2.408). It is worth noting that despite we found the largest U_{equiv} values for oxygen atoms in the water molecules, their ratios longest/shortest axes are only 1.440 to 1.858.

Origin of rapidcreekite

The occurrence of rapidcreekite along with gypsum, tamarugite, and other Al-bearing sulfate efflorescences is a notable feature of the present surficial sulfuric acid weathering environment of the Diana Cave. The peculiar setting responsible for the formation of this mineral assemblage is controlled by 1) the development of the cave along the Diana Fault and 2) a H_2S-rich thermo-mineral water source within the cave. The first condition is crucial in that the downthrown

footwall block of the fault contains marls, which provides the necessary ingredients to produce tamarugite and minerals of the halotrichite group that are part of the rapidcreekite paragenesis. The second factor is responsible for adding to the geochemical system vast amounts of H_2S-charged thermal waters, in which the H_2S is oxidized to H_2SO_4:

$$H_2S + 2O_2 \leftrightarrows 2H^+ + SO_4^{2-} \quad (1)$$

In the case of the Diana Cave, this oxidation occurs in some of the most reducing conditions of the thermal waters of the Cerna Valley, such that the $\delta^{18}O$ values of oxygen in the sulfate ion is derived predominantly from the thermal waters, rather than from atmospheric O_2. Once oxidized, the sulfate ions as well as the abundant H^+ ions reacts with limestone, buffering the acidity of the thermal waters by production of bicarbonate ion. Ultimately this process may drive the solution to gypsum (or anhydrite) saturation according to:

$$2H^+ + SO_4^{2-} + 2CaCO_3 + 2H_2O \rightarrow Ca^{2+} + 2HCO_3^- + CaSO_4 \cdot 2H_2O \quad (2)$$

Work by Dydo et al. (2003) and Schausberger et al. (2009) elucidates the geochemical conditions conducive to rapidcreekite precipitation. These authors have studied the controls of this mixed bicarbonate-sulfate system on carbonate mineral saturation, including equilibrium precipitation of carbonates, sulfates, and mixed carbonate-sulfate minerals such as rapidcreekite. Because rapidcreekite is more soluble than calcite, its precipitation requires low carbonate concentrations relative to sulfate (in experiments of Dydo et al. 2003), when $CO_3^{2-}/SO_4^{2-} = 4.5 \cdot 10^{-3}$). Busenberg and Plummer (1985) described more quantitatively the apparent equilibrium constant of carbonate-sulfate co-precipitates as:

$$Ca_xNa_{(x-1)}CO_{3(y)}SO_{4(1-y)} \leftrightarrows xCa^{2+} + (1 - x)Na^+ + yCO_3^{2-} + (1 - y)SO_4^{2-} \quad (3)$$

$$\log K = \log K_{CaCO3} + 6.3\ ((1-y)/2) + 0.087\ (1-x)/2) \quad (4)$$

296 Thus, log K of rapidcreekite (x = 1, y = 0) is 1.575 higher than that of calcite. Equilibrium
297 modeling of typical sample chemical compositions from Diana 1 and 2 (Constantin, unpubl. data;
298 Ponta, unpubl. data) produces calcite saturation indexes ($SI_{calcite}$) of 0.93-2.25. Given the effect of
299 high sulfate ion activity typical of the Diana Cave, the modeled equilibrium saturation index for
300 rapidcreekite shows that at times the waters are supersaturated with respect to this theoretical
301 rapidcreekite equilibrium constant ($SI_{rapidcreekite}$ = 0.65 to 0.66). Supersaturated conditions occur
302 when the modeled equilibrium CO_3^{2-}/SO_4^{2-} ratio is low (0.06-0.46). As the pH of the solutions rise
303 above 6.4 during gypsum precipitation (reaction 2), the waters may then precipitate rapidcreekite
304 besides a 'Ca-carbonate' mineral:

305 $$3Ca^{2+} + 2HCO_3^- + SO_4^{2-} + 3H_2O \rightarrow Ca_2(SO_4)(CO_3)\cdot 4H_2O + \text{'}CaCO_3\text{'} \quad (5)$$

306 Thus, the controlling factors in the distribution of various types of minerals are the activity of
307 ions available (both in the bedrock and steam-condensed solutions), pH, and the local physical
308 conditions (temperature, relative humidity, cave ventilation). If this interpretation is correct, the
309 narrow stability range of rapidcreekite explains the relatively few observations of the mineral in
310 nature.
311 The 'carbonate phase' formed in reaction (5) could be the one observed during the SEM-EDS
312 scan as aggregates growing on rapidcreekite's crystal faces (Fig. 1b). Given the presence of
313 epsomite ($MgSO_4\cdot 7H_2O$) in the mineral assemblage of the Diana Cave (in the same part of the cave
314 where gypsum and rapidcreekite were identified), we tentatively conclude that the 'carbonate
315 mineral' might be aragonite or even vaterite as Mg^{2+} is known (from nature and laboratory
316 experiments) to promote the growth of either minerals over calcite (Folk 1974; Reddy and
317 Nancollas 1976; Carlson 1983; Kawano et al. 2009; Bots 2011).
318 Consequently, we conclude that rapidcreekite can form simultaneously or shortly after the full

crystallization of gypsum and prior to the growth of the '$CaCO_3$ phase' when both SO_4^{2-} and CO_3^{2-} are present in the system. Due to the presence of limestone and gypsum, which both release Ca^{2+} when they dissolve, we suggest that the common-ion effect may initiate the precipitation of rapidcreekite and be responsible for the deposition of the carbonate phase. The Al sulfates precipitate only when the pH of the steam-condensed fluids drops below 4.5 and favorable ionic activities occur (Martin et al. 1999; Rodgers et al. 2000; Hall et al. 2003). However, it appears that the Al-bearing sulfates form ephemeral efflorescences that may dissolve during cold seasons when relative humidity in the cave atmosphere decreases as dry air enters from outside. An increase of the rain water percolating into the cave will have a similar effect. Both these factors impact the pH at which the sulfate acid reactions happen and thus control the stability and formation of tamarugite, epsomite, and rapidcreekite. Regeneration follows dissolution, once appropriate conditions are restored within the cave.

The $\delta^{34}S$ values of the sulfate samples from the Diana Cave indicate an almost complete, sulfate-limited TSR (high H_2S / SO_4^{2-}) under highly anoxic conditions in the deep thermal water. Such values are consistent with an oxidation of dissolved sulfide in springs of the lower Cerna Valley described by Wynn et al. (2010). This suggests that S in the investigated sulfate minerals is derived from dissolution of primary sulfates from marine limestone followed by reduction in the thermal aquifer and then by re-oxidation in the cave (both in the hot water and atmosphere). The $\delta^{18}O$ values of the sulfate minerals indicate an abundant ^{18}O exchange with $H_2O_{(l)}$ during hydration and near complete exclusion of oxygen derived from $O_{2(aq)}$ in sulfate minerals from the Diana Cave (Onac et al. 2011).

The results presented in this study provide further evidence that rapidcreekite precipitates, and is a persistent mineral phase in the sulfide-rich steam condensate environment of Diana Cave if

342 optimal pH, temperature, ion activity, and relative humidity conditions are met. These conditions,
343 however, are essentially different from other terrestrial records previously documented. Because
344 rapidcreekite was reported from a handful of locations, all different with regard to their geological
345 and physico-chemical parameters, additional information is required before its thermodynamic
346 stability field (for both low or high temperatures) is revealed.
347

348 **Acknowledgements**

349

350 The Domogled-Valea Cernei National Park granted approval to collect samples for analysis. Dr. C.
351 Marin from the Emil Racoviţă Institute of Speleology and G. Ponta (PELA) offered many insights
352 into Cerna Valley hydrochemistry; Vera Dârmiceanu, Lucian Nicoliţă, and Daniel Vereş assisted
353 us during the field campaigns. The authors greatly appreciate the constructive reviews and
354 suggestions from Joel Grice, an anonymous referee, Ron Peterson (Technical Editor), as well as the
355 Associate Editor, Diego Gatta. Type material is deposited in the Mineralogical Museum of the
356 Babeş-Bolyai University in Cluj Napoca, Romania. This work has received financial support from
357 the Romanian National Authority for Scientific Research (grant IDEI_544 to BPO). We dedicate
358 this paper to Prof. Dr. Josef Zemann on the occasion of his 90th birthday anniversary.

359 **References**

360

361 Audra, P. and Hobléa, F. (2007) The first cave occurrence of jurbanite [Al(OH SO_4)·$5H_2O$],
362 associated with alunogen [$Al_2(SO_4)_3$·$17H_2O$] and tschermigite [$NH_4Al(SO_4)_2$·$12H_2O$]:
363 thermal-sulfidic Serpents Cave, France. Journal of Cave and Karst Studies, 69, 243-249.
364 Bernhardt, H.-J. (2010) MINCALC-V5, a non EXCEL based computer program for general
365 electron-microprobe mineral analyses data processing. IMA 2010, 20th International
366 Mineralogical Association Congress, Budapest. Acta Mineralogica Petrographica Abstract
367 Series, 6, p. 869.
368 Bots, P. (2011) Experimental investigations of calcium carbonate mineralogy in past and future
369 oceans, 194 pp. PhD Thesis, The University of Leeds, UK.
370 Busenberg, E. and Plummer, N.L. (1985) Kinetic and thermodynamic factors controlling the
371 distribution of SO_4^{2-} and Na^+ in calcites and selected aragonites. Geochimica et Cosmochimica
372 Acta, 49, 713-725.
373 Carlson, W.D. (1983) The polymorphs of $CaCO_3$ and the aragonite-calcite transformation. In R.J.
374 Reeder, Ed., Carbonates: mineralogy and chemistry, 11, p. 191-225, Reviews in Mineralogy,
375 Mineralogical Society of America, Chantilly, Virginia.
376 Cooper, M.A. and Hawthorne, F.C. (1996) The crystal structure of rapidcreekite,
377 $Ca_2(SO_4)(CO_3)(H_2O)_4$, and its relation to the structure of gypsum. Canadian Mineralogist, 34,
378 99-106.
379 Cosma, C., Suciu, I., Jäntschi, L., and Bolboacă, S.D. (2008) Ion-molecule reactions and chemical
380 composition of emanated from Herculane Spa geothermal sources. International Journal of
381 Molecular Sciences, 9, 1024-1033.

Demartin, F., Castellano, C., Gramaccioli, C.M., and Campostrini, I. (2010) Aluminocoquimbite, $AlFe(SO_4)_3 \cdot 9H_2O$, a new aluminum iron sulphate from Grotta Dell'Allume, Vulcano, Aeolian Islands, Italy. Canadian Mineralogist, 48, 1465-1468.

Diaconu, G. (1974) Quelques considérations sur la présence de l'anhydrite dans la grotte "Pestera Diana" (Băile Herculane-Roumanie). Travaux Institute Spéologie "Emile Racovitza", 13, 191-194.

Diaconu, G. and Medeşan, A. (1973) Sur la présence de pickeringite dans la grotte Diana (Băile Herculane, Roumanie). Travaux Institute Spéologie "Emile Racovitza", 12, 303-309.

Dowty, E. (1999) ATOMS 5.0, a computer program. Kingsport, TN.

Dydo, P., Turek, M., and Ciba, J. (2003) Scaling analysis of nanofiltration systems fed with saturated calcium sulfate solutions in the presence of carbonate ions. Desalination, 159, 245-251.

Effenberger, H. and Langhof, H. (1984) On the planarity of the CO_3 group in buetschliite, dipotassium calcium dicarbonate, $K_2Ca(CO_3)_2$. Acta Crystallographica, C40, 1299-1300.

Effenberger, H., Mereiter, K., and Zemann, J. (1981) Crystal structure refinements of magnesite, calcite, rhodochrosite, siderite, smithonite, and dolomite, with discussion of some aspects of the stereochemistry of calcite type carbonates. Zeitschrift für Kristallographie, 156, 233-243.

Folk, R.L. (1974) The natural history of crystalline calcium carbonate: effect of magnesium content and salinity. Journal of Sedimentary Petrology, 44, 40-53.

Forti, P., Panzica La Manna, M., and Rossi, A. (1996) The peculiar mineralogical site of the Alum cave (Vulcano, Sicily). In P. Oromí, Ed., 7th International Symposium on Vulcanospeleology, p. 35-44, Canary Islands, November 1994.

Galdenzi, S. and Maruoka, T. (2003) Gypsum deposits in the Frasassi Caves, Central Italy. Journal of Cave and Karst Studies, 65, 111-125.

Galdenzi, S., Cocchioni, F., Filipponi, G., Morichetti, L., Scuri, S., Selvaggio, R., and Cocchioni, M. (2010) The sulfidic thermal caves of Acquasanta Terme (central Italy). Journal of Cave and Karst Studies, 72, 43-58.

Gatta, G.D., McIntyre, G.J., Swanson, J.G., and Jacobsen, S.D. (2012) Minerals in cement chemistry: A single-crystal neutron diffraction and Raman spectroscopic study of thaumasite, $Ca_3Si(OH)_6(CO_3)(SO_4)\cdot 12H_2O$. American Mineralogist, 97, 1060-1069.

Grassineau, N., Mattey, D., and Lowry, D. (2001) Sulfur isotope analysis of sulfide and sulfate minerals by continuous low-isotope ratio mass spectrometry. Analytical Chemistry, 73, 220-225.

Hall, A.J., Fallick, A.E., Perdikatsis, V., and Photos-Jones, E. (2003) A model for the origin of Al-rich efflorescences near fumaroles, Melos, Greece: enhanced weathering in a geothermal setting. Mineralogical Magazine, 67, 363-379.

Hill, C.A. and Forti, P. (1997) Cave minerals of the world, 2nd ed., 463 p. National Speleological Society, Huntsville, Alabama.

Hose, L.D., Palmer, A.N., Palmer, M.V., Northup, D.E., Boston, P.J., and DuChene, H.R. (2000) Microbiology and geochemistry in a hydrogen-sulphide-rich karst environment. Chemical Geology, 169, 399-423.

Kawano, J., Shimobayashi, N., Miyake, A., and Kitamura, M. (2009) Precipitation diagram of calcium carbonate polymorphs: its construction and significance. Journal of Physics: Condensed Matter, 21, 425102.

Lazaridis, G., Melfos, V., and Papadopoulou, L. (2011) The first cave occurrence of orpiment (As_2S_3) from the sulphuric acid caves of Aghia Paraskevi (Kassandra Peninsula, N. Greece). International Journal of Speleology, 40, 133-139.

Marin, C. (1984) Hydrochemical considerations in the lower Cerna river basin. Theoretical and Applied Karstology, 1, 173-182.

Martin, R., Rodgers, K.A., and Browne, P.R.L. (1999) The nature and significance of sulphate-rich, aluminous efflorescences from the Te Kopia geothermal field, Taupo Volcanic Zone, New Zealand. Mineralogical Magazine, 63, 413-419.

Martínez-Ramírez, S. and Fernández-Carrasco, L. (2012) Carbonation of ternary cement systems. Construction and Building Materials, 27, 313-318.

Năstăseanu, S.V. (1980) Géologie des Monts Cerna. Anuarul Institutului de Geologie şi Geofizică, LIV, 153-280.

Nehring, N.L., Bowen, P.A., and Truesdell, A.H. (1977) Technique for the conversion to carbon dioxide of oxygen from dissolved sulfate in thermal waters. Geothermics, 5, 63-66.

Nonius, B.V. (1999) "Collect". Data collection software. Brucker AXS, http://www.brucker-axs.de/

Onac, B.P. (2012) Minerals. In W.B. White and D.C. Culver, Eds., Encyclopedia of Caves, p. 499-508. Academic Press, Chennai.

Onac, B.P. and Forti, P. (2011a) Minerogenetic mechanisms occurring in the cave environment: an overview. International Journal of Speleology, 40, 79-98.

Onac, B.P. and Forti, P. (2011b) State of the art and challenges in cave minerals studies. Studia UBB Geologia, 56, 33-42.

Onac, B.P., Sumrall, J., Tămaş, T., Cizmaş, C., Dârmiceanu, V., Povară, I., and Nicolită, L. (2009a) Mineralogical and stable isotope investigations of minerals from caves on Cerna Valley (Romania). In W.B. White, Ed., Proceedings of the 15th International Congress of Speleology, 1, p. 318-323. Kerrville, Texas.

448 Onac, B.P., Sumrall, J., Tămaş, T., Povară, I., Kearns, J., Dârmiceanu, V., Vereş, D., and Lascu, C.
449 (2009b) The relationship between cave minerals and hypogene activity along the Cerna Valley
450 (SW Romania). Acta Carsologica, 38, 67-79.
451 Onac, B.P., Wynn, J.G., and Sumrall, J.B. (2011) Tracing the sources of cave sulfates: a unique
452 case from Cerna Valley, Romania. Chemical Geology, 288, 105-114.
453 Otwinowski, Z. and Minor, W. (1997) Processing of X-ray diffraction data collected in oscillation
454 mode. In C.W.J. Carter and R.M. Sweet, Eds., Methods in Enzymology, 276, p. 307-326.
455 Parkhurst D.L. and Appelo C.A.J. (1999) User's guide to PHREEQC (Version 2) – a computer
456 program for speciation, batch-reaction, one-dimensional transport, and inverse geochemical
457 calculations. U.S. Geological Survey Water Resources Investigations Report 99-4259, 312 p.
458 Povară, I. (2001) Thermal springs in Băile Herculane (Romania). In P.E. LaMoreaux and J.T.
459 Tanner, Eds., Spring and bottled waters of the world: Ancient history, source, occurrence,
460 quality, and use, p. 210-216. Springer, Berlin.
461 Povară, I., Diaconu, G., and Goran, C. (1972) Observations préliminaires sur les grottes
462 influencées par les eaux thermo-minérales de la zone Băile-Herculane. Travaux Institute
463 Spéologie "Emile Racovitza", 11, 355-365.
464 Povară, I, Simion, G., and Marin, C. (2008). Thermo-mineral waters from the Cerna Valley Basin
465 (Romania). Studia UBB Geologia, 53, 41-54.
466 Puşcaş, C.M., Onac, B.P., Effenberger, H.S., and Povară, I. (2013) Tamarugite-bearing paragenesis
467 formed by sulphate acid alteration in Diana Cave, Romania. European Journal of Mineralogy,
468 DOI: 10.1127/0935-1221/2013/0025-2294.
469 Raade, G. (1989) "Etter Neumann". NAGS-nytt, 16(2), 49.
470 Reddy, M.M. and Nancollas, G.H. (1976) The crystallisation of calcium carbonate: IV. The effect
471 of magnesium, strontium, and sulfate ions. Journal of Crystal Growth, 35, 33-38.

Roberts, A.C., Ansell, H.G., Jonasson, I.R., Grice, J.D., and Ramik, R.A. (1986) Rapidcreekite, a new hydrated calcium sulfate-carbonate from the Rapid Creek area, Yukon Territory. Canadian Mineralogist, 24, 51-54.

Rodgers, K.A., Hamlin, K.A., Browne, P.R.L., Campbell, K.A., and Martin, R. (2000) The steam condensate alteration mineralogy of Ruatapu cave, Orakei Korako geothermal field, Taupo Volcanic Zone, New Zealand. Mineralogical Magazine, 64, 125-142.

Rüger, F., Senf, L., and Witzke, T. (1995) Die Saalfelder Feengrotten: Seltene Sekundärmineralien aus Thüringen. Lapis, 20(1), 15-26.

Schausberger, P., Mustafa, G.M., Leslie, G., and Friedl, A. (2009) Scaling prediction based on thermodynamic equilibrium calculation - scopes and limitations. Desalination, 244, 31-47.

Schmid, S.M., Berza, T., Diaconescu, V., Froitzheim, N., and Fügenschuh, B. (1998) Orogen-parallel extension in the Southern Carpathians. Tectonophysics, 297, 209-228.

Sheldrick, G.M. (1997) SHELXL-97, a program for crystal structure refinement. University of Göttingen, Germany.

Sheldrick, G.M. (2008) A short history of SHELX. Acta Crystallographica, A64, 112-122.

Spallanzani, L. (1797) Viaggi alle Due Sicilie ed in alcune parti dell'Appennino, 2, 202-206.

Walenta, K. and Dunn, P.J. (1989) Camgasit, ein neues Calcium-Magnesiumarsenatmineral der Zusammensetzung $CaMg(AsO_4)(OH)\cdot 5H_2O$ von Wittichen im mittleren Schwarwald. Aufschluss, 40, 369-372.

Wynn, J.G., Sumrall, J.G., and Onac, B.P. (2010) Sulfur isotopic composition and the source of dissolved sulfur species in thermo-mineral springs of the Cerna Valley, Romania. Chemical Geology, 271, 31-43.

Žák K., Skála R., Filippi M., and Plášil J. (2010) Ikaite - little known mineral of iced caves: occurence in seasonal cave ice formations of the Koda Cave (Bohemian Karst). Bulletin mineralogicko-petrologického oddělení Národního muzea v Praze, 18, 109-115 (In Czech).

Zemann, J. (1981) Zur Strukturchemie der Karbonate. Fortschritte der Mineralogie, 89, 95-116.

499 **Figures caption**

500 **Figure 1.** SEM image of bundle rapidcreekite crystals (**a**) and details showing the EDS-confirmed
501 carbonate phase growing on their crystal surface (**b**).

502

503 **Figure 2.** The crystal structure of rapidcreekite (program ATOMS; Dowty 1999).

504

505 **Figure 3.** The surrounding of the carbonate group in rapidcreekite causing its aplanarity (program
506 ATOMS; Dowty 1999).

507

508 Table 1. $\delta^{34}S$ and $\delta^{18}O$ values for rapidcreekite (*) and bulk sulfate (§) minerals from Diana Cave,

509 Romania

Sample #	Mineral habit	$\delta^{34}S$ (‰)	$\delta^{18}O$ (‰)
1770a *	efflorescence	19.3	-8.7
1770b§	efflorescence	19.4	-8.7
1771a*	efflorescence	18.0	-9.1
1771b§	efflorescence	18.3	-9.1
1772§	efflorescence	18.7	-9.1
1773a*	efflorescence	19.1	-9.3
1773b§	efflorescence	19.2	-9.5
1775*	crust	19.5	-9.7
1776§	crust	19.2	-7.8
1777§	efflorescence	18.8	-9.4

510

Table 2. Summary of single-crystal X-ray data† and structure refinements of rapidcreekite

a [Å]	15.524(2)
b [Å]	19.218(3)
c [Å]	6.161(1)
Space group	*Pcnb*
V [Å^3]	1838.1(5)
Z	8
ρ_{calc} [g cm^{-3}] / μ(Mo$K\alpha$) [mm^{-1}]	2.23 / 1.5
Range of data collection ($\pm h$ $\pm k$ $\pm l$) [°]	$3 < 2\vartheta < 65$
Number of images / rotation angle per image [°]	1141 / 1
Scan mode (at 11 distinct ω-angles)	φ-scans
Scan time [s/°] / frame size (binned mode)	120 / 621×576 pixels
Detector-to-sample distance [mm]	40
Measured reflections	29,694
Unique reflections (n) / reflections with $F_o > 4\sigma(F_o)$	3,331 / 2,592
$R_{int} = \Sigma \lvert F_o^2 - F_o^2(\text{mean}) \rvert / \Sigma F_o^2$	0.058
$R1 = \Sigma(\lvert \lvert F_o \rvert - \lvert F_c \rvert \rvert) / \Sigma F_o$ (3,331 / 2,592 reflections)	0.048 / 0.030
$wR2 = [\Sigma w(F_o^2 - F_c^2)^2 / \Sigma \lvert wF_o^4]^{1/2}$	0.080
GooF = $\{\Sigma[w(F_o^2 - F_c^2)^2] / (n-p)\}^{0.5}$	1.059
Max Δ/σ; number of variable parameters (p)	< 0.001; 162
Final difference Fourier map [eÅ^{-3}]	-0.48 to +0.46

Notes: $w = 1 / \{ \sigma^2(F_o^2) + [0.045 \times P]^2 + 0.17 \times P \}$; $P = ([\max(0, F_o^2)] + 2 \times F_c^2) / 3]$.
†NONIUS four-circle diffractometer equipped with a CCD detector and a 300 μm capillary-optics collimator (Mo tube, graphite monochromator). Unit-cell parameters were obtained by least-squares refinements of 2ϑ values. Data were corrected for background, Lorentz, polarization, and absorption effects (multi-scan method; complex scattering functions). Extinction was not observed. Programs used: COLLECT (Nonius 1999; Otwinowski and Minor 1997) and SHELXL-97 (Sheldrick 1997; 2008).

Table 3. Fractional atomic coordinates and displacement parameters of rapidcreekite

Atom	*x*	*y*	*z*	U_{equiv} / U_{iso}	U_{11}	U_{22}	U_{33}	U_{23}	U_{13}	U_{12o}
Ca1	0.334002(18)	0.289513(15)	0.20090(5)	0.01712(8)	0.01787(14)	0.01618(14)	0.01733(14)	-0.00086(10)	-0.00016(10)	-0.00035(10)
Ca2	0.327543(18)	0.053335(15)	0.18898(5)	0.01655(8)	0.01821(14)	0.01593(14)	0.01552(14)	0.00084(10)	0.00018(10)	0.00052(10)
S	0.16871(2)	0.419309(18)	0.02690(6)	0.01621(9)	0.01788(16)	0.01490(16)	0.01584(16)	-0.00090(12)	0.00004(12)	-0.00009(11)
C	0.19103(10)	0.17345(7)	0.4337(2)	0.0165(3)	0.0175(6)	0.0180(6)	0.0140(6)	0.0000(5)	-0.0007(5)	-0.0001(5)
O1	0.22452(7)	0.35836(6)	0.04875(19)	0.0250(2)	0.0278(5)	0.0202(5)	0.0268(6)	0.0006(4)	-0.0030(4)	0.0069(4)
O2	0.21343(7)	0.23291(5)	0.35720(18)	0.0204(2)	0.0235(5)	0.0166(5)	0.0212(5)	0.0020(4)	0.0030(4)	-0.0019(4)
O3	0.38966(7)	0.40374(6)	0.34196(18)	0.0239(2)	0.0254(5)	0.0229(5)	0.0235(6)	-0.0039(4)	0.0063(4)	-0.0011(4)
O4	0.37085(7)	0.17133(5)	0.07484(18)	0.0191(2)	0.0193(5)	0.0193(5)	0.0187(5)	0.0004(4)	-0.0034(4)	-0.0009(4)
O5	0.22870(7)	0.11704(5)	0.38274(18)	0.0243(2)	0.0299(6)	0.0191(5)	0.0239(5)	0.0012(4)	0.0093(5)	0.0048(4)
O6	0.28117(7)	0.48285(5)	0.48411(18)	0.0228(2)	0.0255(5)	0.0186(5)	0.0243(6)	-0.0012(4)	-0.0050(4)	0.0045(4)
O7	0.11778(7)	0.43255(6)	0.22415(18)	0.0242(2)	0.0277(6)	0.0232(5)	0.0217(5)	-0.0031(4)	0.0070(4)	-0.0029(4)
W1	0.08933(8)	0.23878(7)	0.0107(2)	0.0274(3)	0.0269(6)	0.0318(6)	0.0235(6)	0.0007(5)	0.0000(5)	-0.0040(5)
W2	0.04803(8)	0.32244(7)	0.4660(2)	0.0296(3)	0.0243(6)	0.0308(7)	0.0336(7)	0.0061(5)	-0.0049(5)	0.0004(5)
W3	0.07520(8)	0.02078(7)	0.3958(2)	0.0252(2)	0.0247(6)	0.0274(6)	0.0236(6)	-0.0041(5)	-0.0004(5)	-0.0006(5)
W4	0.43354(9)	0.09068(8)	0.4675(2)	0.0288(3)	0.0250(6)	0.0334(7)	0.0280(6)	0.0030(5)	-0.0040(5)	-0.0018(5)
$H_{Ow1\text{-}Ow1}$	0.0414(16)	0.2390(16)	0.033(4)	0.045(4)*						
$H_{Ow1\text{-}O2}$	0.1182(16)	0.2440(14)	0.116(5)	0.045(4)*						
$H_{Ow2\text{-}O4}$	0.003(2)	0.3337(14)	0.485(6)	0.045(4)*						
$H_{Ow2\text{-}O7}$	0.0623(19)	0.3598(15)	0.402(5)	0.045(4)*						
$H_{Ow3\text{-}Ow3}$	0.0372(18)	0.0193(17)	0.427(5)	0.045(4)*						
$H_{Ow3\text{-}O3}$	0.0906(17)	-0.0138(14)	0.338(5)	0.045(4)*						
$H_{Ow4\text{-}O3}$	0.4914(19)	0.1012(15)	0.425(5)	0.045(4)*						
$H_{Ow4\text{-}Ow1/Ow3}$	0.437(2)	0.0917(17)	0.553(5)	0.045(4)*						

Notes: Anisotropic displacement parameters: exp [$-2\pi^2 \Sigma^3_{i=1} \Sigma^3_{j=1} U_{ij} a^*_i a^*_j h_i h_j$]; * constrained during refinement.

Table 4. Interatomic bond lengths (Å) and bond angles (°) for rapidcreekite

Ca1—O1	2.3491(11)	Ca2—O5	2.2975(11)
Ca1—O2	2.3695(11)	Ca2—O6^{v}	2.4124(11)
Ca1—O_W2^{iii}	2.4183(13)	Ca2—O5^{iii}	2.4126(11)
Ca1— O_W1^{iv}	2.4517(13)	Ca2— O_W3^{iii}	2.4360(13)
Ca1—O4	2.4675(10)	Ca2—O4	2.4676(10)
Ca1—O2^{iii}	2.4919(11)	Ca2— O_W4	2.4837(13)
Ca1—O3	2.5142(12)	Ca2—O7^{v}	2.5289(11)
Ca1—O1^{iv}	2.6775(12)	Ca2—O6^{viii}	2.5318(12)
S—O1	1.4631(11)	C—O5	1.2712(17)
S—O6^{iii}	1.4718(11)	C—O2	1.2839(17)
S—O7	1.4719(11)	C—O4^{iv}	1.2964(18)
S—O3^{iii}	1.4862(11)		

Hydrogen bonds

Donor	H atom	Acceptor	D—H	H···A	D···A	D—H···A	H···D···H	A···D···A	A···H···A
O_w1	$H_{Ow1\text{-}Ow1}$	O_w1^{i}	0.76(3)	2.08(3)	2.807(2)	162(3)			
O_w1	$H_{Ow1\text{-}O2}$	O2	0.80(3)	2.11(3)	2.878(2)	163(3)	113(3)	131.88(3)	
O_w2	$H_{Ow2\text{-}O4}$	O4^{vi}	0.74(3)	2.13(3)	2.834(2)	160(3)			
O_w2	$H_{Ow2\text{-}O7}$	O7	0.85(3)	1.98(3)	2.806(2)	166(3)	94(3)	117.94(5)	
O_w3	$H_{Ow3\text{-}Ow3}$	O_w3^{vii}	0.62(3)	2.20(3)	2.782(2)	157(4)			
O_w3	$H_{Ow3\text{-}O3}$	O3^{v}	0.79(3)	1.96(3)	2.739(2)	169(3)	113(3)	100.27(7)	
O_w4	$H_{Ow4\text{-}O3}$	O3^{ii}	0.96(3)	1.92(5)	2.854(2)	165(3)			
O_w4	$H_{Ow4\text{-}Ow1/Ow3}$	O_w1^{iv}	0.53(3)	2.87(3)	2.881(2)	86(4)	96.11(5)		
O_w4	$H_{Ow4\text{-}Ow1/Ow3}$	O_w3^{iv}	0.53(3)	2.52(3)	2.964(2)	144(4)	100(4)	107.61(5)	127(1)

Note: Symmetry code: not specified and ^{0} *x,y,z*; ^{i} -*x*,-*y*+½,*z*; ^{ii} -*x*+1,-*y*+½,*z*; ^{iii} -*x*+½,*y*,*z*-½; ^{iv} -*x*+½,*y*,*z*+½; ^{v} -*x*+½,*y*-½,-*z*+½; ^{vi} *x*-½,-*y*+½,*z*+½; ^{vii} -*x*,-*y*,-*z*+1; ^{viii} *x*,*y*-½,-*z*+1.

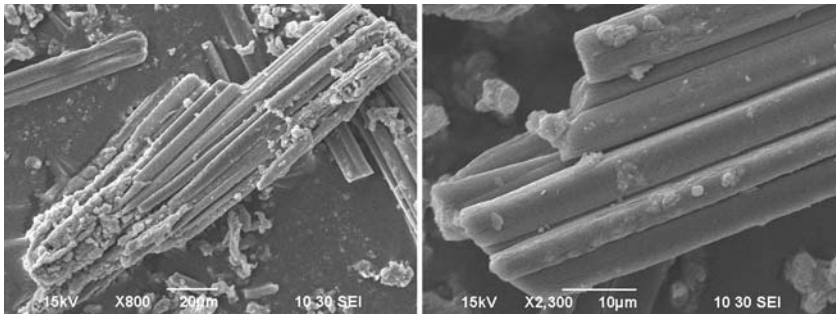
15kV X800 20µm 10 30 SEI
15kV X2,300 10µm 10 30 SEI

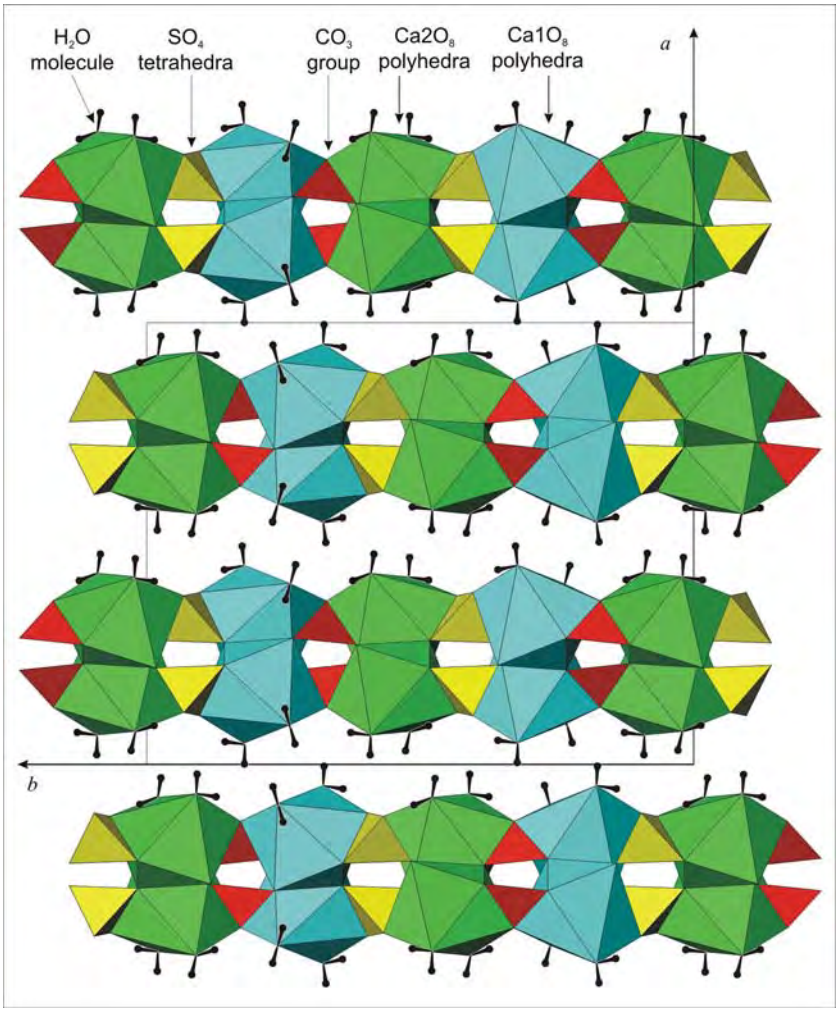
H_2O molecule
SO_4 tetrahedra
CO_3 group
$Ca2O_8$ polyhedra
$Ca1O_8$ polyhedra
a
b

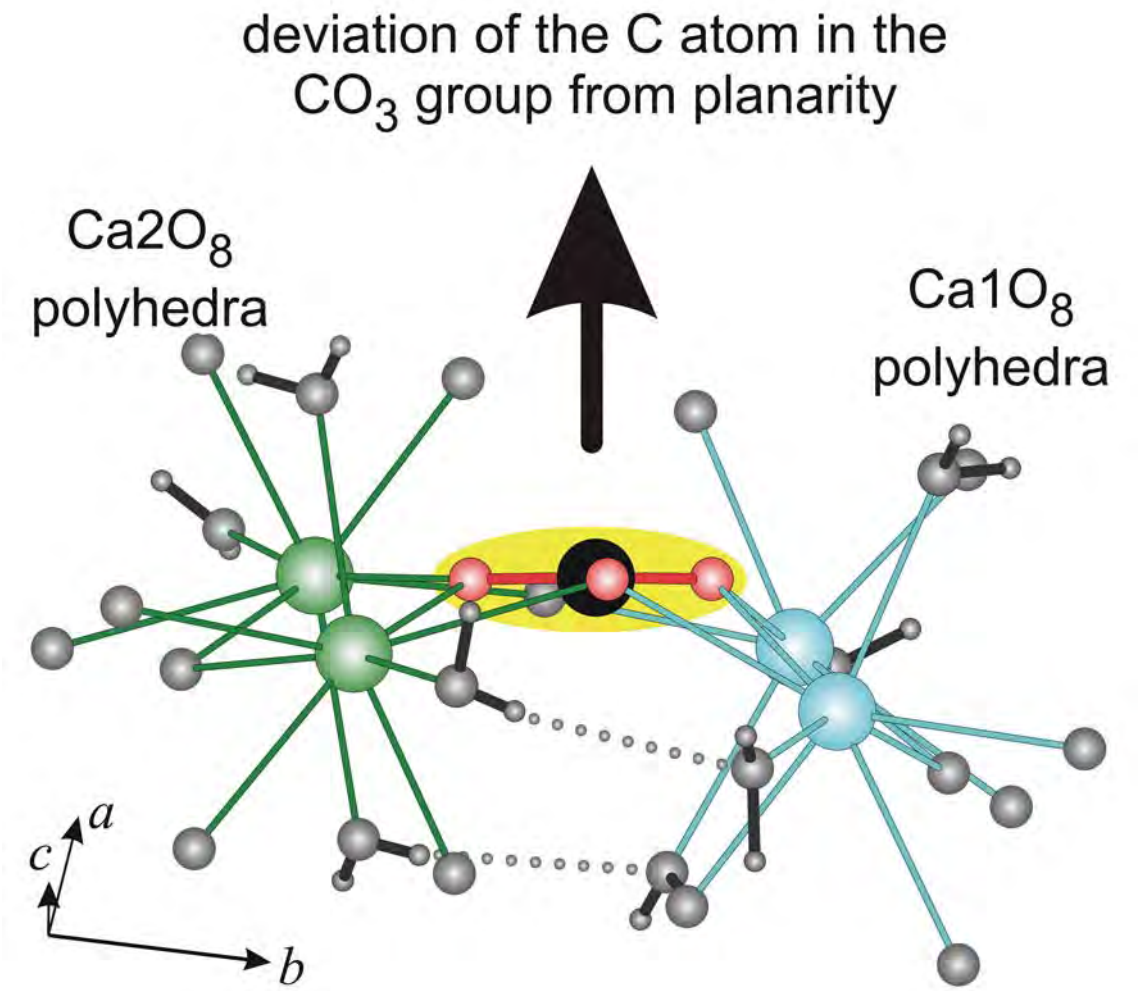
deviation of the C atom in the
CO_3 group from planarity
$Ca2O_8$
polyhedra
$Ca1O_8$
polyhedra
a
c
b